

South Equatorial Current of the Indian Ocean: a fifty-day oscillation

Fifty-day oscillation
Rossby wave
Indian Ocean
Currents
CZCS

Oscillation d'une période de cinquante jours
Onde de Rossby
Océan Indien
Courants
CZCS

Karen J. HEYWOOD*, Eric D. BARTON and Graham L. ALLEN

School of Ocean Sciences, University College of North Wales, Menai Bridge,
Gwynedd LL59 5EY, UK.

* *Present address*: School of Environmental Sciences, University of East Anglia,
Norwich NR4 7TJ, UK.

Received 24/06/93, in revised form 3/01/94, accepted 11/02/94.

ABSTRACT

Observations of a fifty-day oscillation in the meridional component of the South Equatorial Current in the Western Indian Ocean are presented. Currents measured in 4000 m of water close to the atoll of Aldabra (46°E, 9°S) reveal the oscillation throughout the water column to a depth of 3000 m. Further evidence of the oscillation is presented in shipboard Acoustic Doppler Current Profiler (ADCP) sections and in Coastal Zone Color Scanner (CZCS) imagery. The oscillations are consistent with a zonally propagating Rossby wave caused by shear instability in the zonal flow of the South Equatorial Current.

Oceanologica Acta, 1994. 17, 3, 255-261.

RÉSUMÉ

Courant sud-équatorial de l'Océan Indien : oscillation d'une période de cinquante jours

Une oscillation dont la période est de cinquante jours a été observée dans la composante méridienne du courant sud-équatorial, dans l'ouest de l'Océan Indien. Dans la colonne d'eau de 4000 m adjacente à l'atoll d'Aldabra (46 °E, 9 °S), la courantométrie révèle la présence d'une oscillation jusqu'à 3000 m de profondeur. Une autre preuve de cette oscillation est apportée par les profils de courantométrie acoustique Doppler (ADCP) et par la télédétection satellitale CZCS. Les oscillations observées sont en accord avec la propagation zonale de l'onde de Rossby produite par l'instabilité du cisaillement dans l'écoulement du courant sud-équatorial.

Oceanologica Acta, 1994. 17, 3, 255-261.

INTRODUCTION

Dominant features of the Indian Ocean include strong variability of currents on a range of time scales. The monsoon winds drive seasonal current reversals along the African and Arabian coasts (Luther and O'Brien, 1985) as well as at the equator (Wyrki, 1973). The South Equatorial Current variation on the same time scale is documented by

Cutler and Swallow (1984). Current oscillations on shorter time scales of weeks to months have been noted by Luyten and Roemmich (1982) near the African coast and by Quadfasel and Swallow (1986) and Schott *et al.* (1988) off Madagascar. Schott *et al.* (1988) report fluctuations with a forty- to fifty-day period in the boundary current transports off the east coast of Madagascar. An oscillation with a period of forty to sixty days has been reported in the long

shore currents of the Somali current off the Kenyan coast (Mysak and Mertz, 1984). Quadfasel and Swallow (1986) present current meter data from a site off the northern tip of Madagascar during March-July 1975 which indicate a fifty-day period oscillation with an amplitude of 12 cm s^{-1} . They also report meanders of a similar amplitude and wavelength about 400 km in surface current vectors.

As part of a study of flow disturbance by oceanic islands (Heywood *et al.*, 1990), two current meter moorings were deployed in deep water (4000 m) west of the coral atoll of Aldabra (Fig. 1). Current records from these moorings, located at 10°S in the South Equatorial Current, show evidence of a fifty-day oscillation in the meridional component down to some 3000 m below surface. Further evidence of current oscillations on a similar scale in the upper layers can be seen in transects of acoustic Doppler current profiler (ADCP) measurements and in Coastal Zone Color Scanner (CZCS) imagery.

Such waves may have important consequences for the biological productivity of the area, and more particularly for some of the isolated islands. We shall show that waves are clearly defined on a front between low chlorophyll content water to the north, and greener water to the south, as shown by surface chlorophyll concentration revealed by ocean colour imagery. A regular influx of a greater phytoplankton population may influence the ecology associated with an island, such as Aldabra, by enhancing the growth of zooplankton and higher organisms.

CURRENT METER OBSERVATIONS

Two current meter moorings, W1 and W2, were deployed in 4000 m of water to the northwest of Aldabra ($46^\circ 20' \text{ E}$, $9^\circ 25' \text{ S}$; Fig. 1) from RRS *Charles Darwin* in late April 1987 and retrieved early in July 1987, approximately eleven weeks later. Six Aanderaa current meters were deployed at each mooring, although battery failure led to

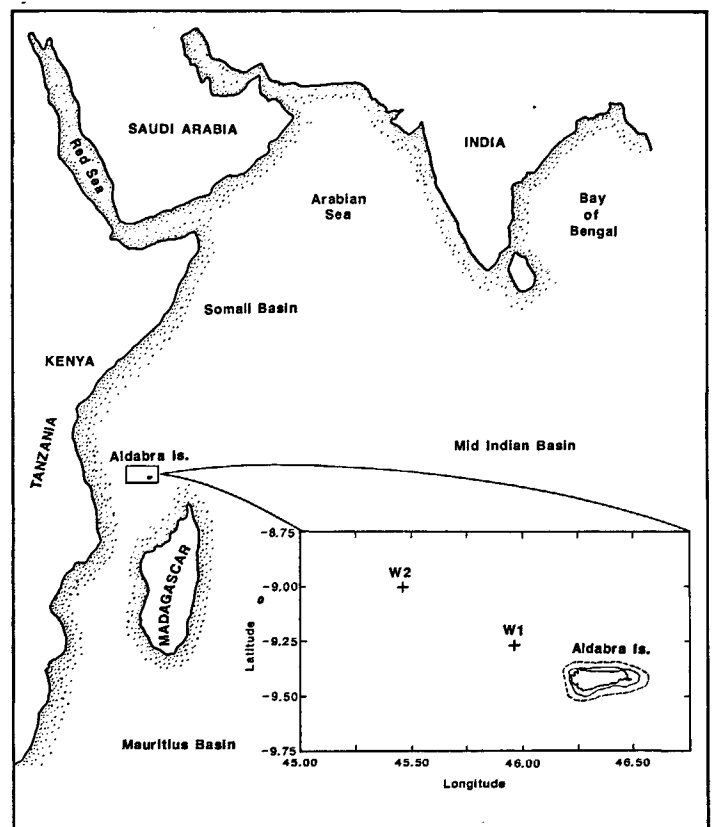


Figure 1

Location of the two moorings, W1 and W2, around the coral atoll of Aldabra. Depth contour of 1000 m is shown as a dashed line in the inset.

the loss of some data sets. The data were edited to eliminate spikes, rotated by 6° to correct for the magnetic deviation from true north, and low-pass filtered using a Cosine-Lanczos 131-point filter with a half-power point at 40 hours in order to eliminate tidal and other high frequency variability. During filtering, the data were decimated to six-hourly values. As attention is focused on low frequency phenomena, the data were further filtered by applying a 21-point running-mean filter, removing oscillations with period less than five days.

The mooring positions, post-filter data record lengths, means and standard deviations of the current components are shown in Table 1. The prevailing near-surface current is westward (W2) or northwestward (W1) as one would expect for the South Equatorial Current during the austral autumn and winter. The standard deviations of the meridional components are considerably larger than the means. This implies the possibility of a significant oscillation in this component.

At W1 a clear fifty-day oscillation, primarily in the meridional component, is seen at 500 m (Fig. 2). What appears to be part of a similar oscillation is evident at 300 m; the signal is in phase between the two levels and has the same amplitude, around 10 cm s^{-1} . The low-frequency oscillation is barely evident at the two uppermost levels. At W2, an oscillation of the same period is seen at all levels (Fig. 3), although higher frequency fluctuations also influence the upper two levels. The oscillation is evident even at the deepest observed level with the same frequency

Table 1

Statistics of the filtered time series from current meter moorings W1 and W2.

Moorings	Depth (m)	Length of data (days)	Zonal mean (cm s^{-1})	Component std dev. (cm s^{-1})	Meridional mean (cm s^{-1})	Component std dev. (cm s^{-1})	
W1	60	69	-3.9	6.8	3.9	5.6	
	$9^\circ 16' \text{ S}$	110	-3.9	8.1	0.8	6.0	
	$45^\circ 58' \text{ E}$	300	39	5.3	5.2	-3.6	6.9
		500	69	3.0	5.8	-3.3	6.6
	3000	8	-6.4	1.0	-5.3	1.3	
W2	80	69	-17.0	10.9	-0.6	11.4	
	$9^\circ 0' \text{ S}$	130	-12.5	12.5	-1.0	10.5	
	$45^\circ 27' \text{ E}$	330	69	-1.5	13.9	-3.9	12.5
		480	69	2.2	9.6	-6.0	10.3
		1000	69	2.5	4.7	-4.2	6.5
		3000	69	-0.8	2.9	1.5	3.4

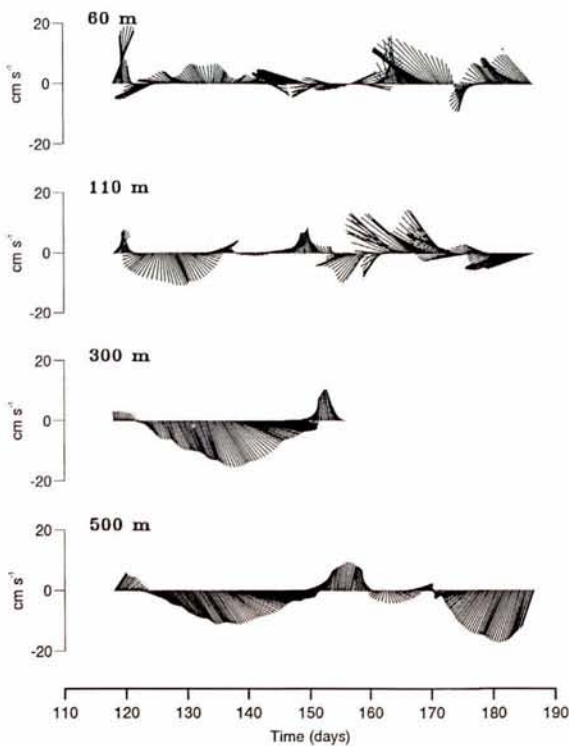


Figure 2

Current vector time series at mooring W1 at the depths shown. Northward currents point up the page. These data have been smoothed and filtered as described in the text.

and period. The amplitude of the oscillation decreases from about 20 cm s^{-1} above 330 m to less than 10 cm s^{-1} at 3000 m. The phase at the deepest level, however, is 180° with respect to all other levels and the mean flow direction is also reversed (Tab. 1). Although we initially suspected instrumental error, we do not believe this to be the case; a current meter record also at 3000 m at mooring W1 ended prematurely after only two weeks, but is sufficiently long to indicate the same 180° phase reversal between the currents above 1000 m and those at 3000 m. This suggests a baroclinic component to the wave. Note that the presence of the oscillation at this great depth is unprecedented.

The temperature time series (not shown) of the two upper current meters at both moorings exhibit an oscillation with a period of the order of 25 days. The amplitude of the oscillation is about 4°C and is consistent with the explanation that the current meters are pulled down by the lateral straining due to the currents. Pressure sensors on several meters indicated that vertical displacements were usually less than 10 m but on two occasions were as large as 20 m during periods of stronger currents. Although this vertical motion does affect the temperature signals, it has negligible effect on the oscillation observed in the current measurements themselves since there is relatively little shear.

EMPIRICAL ORTHOGONAL FUNCTIONS

Empirical Orthogonal Functions (Kundu *et al.*, 1975) were calculated for each of the current components at both

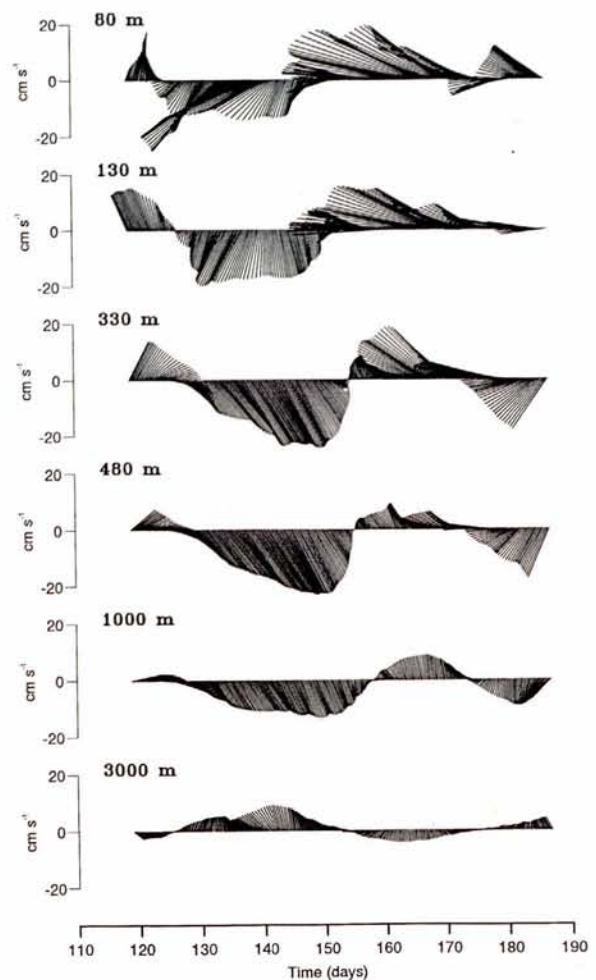


Figure 3

Current vector time series at mooring W2.

moorings separately, weighting each record equally. The EOFs of the zonal components showed no evidence of the oscillation and so are not discussed further. At W1, the two shorter records are omitted from the EOF calculations, so the components at W1 are decomposed into three orthogonal modes. The EOFs calculated for the current components at W2 are each based on the records from all six depths, yielding six modes. Almost all of the variance is explained by modes 1 and 2.

At mooring W2 the meridional component is dominated by the first mode, which accounts for almost 90 % of the total variance (Tab. 2) and clearly shows the fifty-day oscillation (Fig. 4). The vertical structure of mode 1 (Fig. 5) shows only a slight reduction in the magnitude of the eigenfunctions with depth. Mode 2 appears baroclinic with a zero crossing at 250 m, has a periodicity of around 25 days but is not significant because it contributes only 7 % of the total variance.

Fewer data at W1 produce less clear results than at W2, but common characteristics are still evident. The first mode, which accounts for only 50 % of the variance, reveals the fifty-day oscillation but higher frequency fluctuations modify the low frequency signal (Fig. 4). The second mode is similar to that at W2 but is more

Table 2

Empirical orthogonal functions at current meter moorings W1 and W2.

Mooring W1		Mode 1	Mode 2
Explained variance (%)		50	37
Eigenfunction	60 m	0.33	-0.67
	110 m	0.68	-0.32
	500 m	0.65	0.67
Mooring W2		Mode 1	Mode 2
Explained variance		90	7
Eigenfunction	80 m	0.47	-0.75
	130 m	0.45	-0.25
	330 m	0.54	0.41
	480 m	0.44	0.43
	1 000 m	0.26	0.13
	3 000 m	-0.14	-0.12

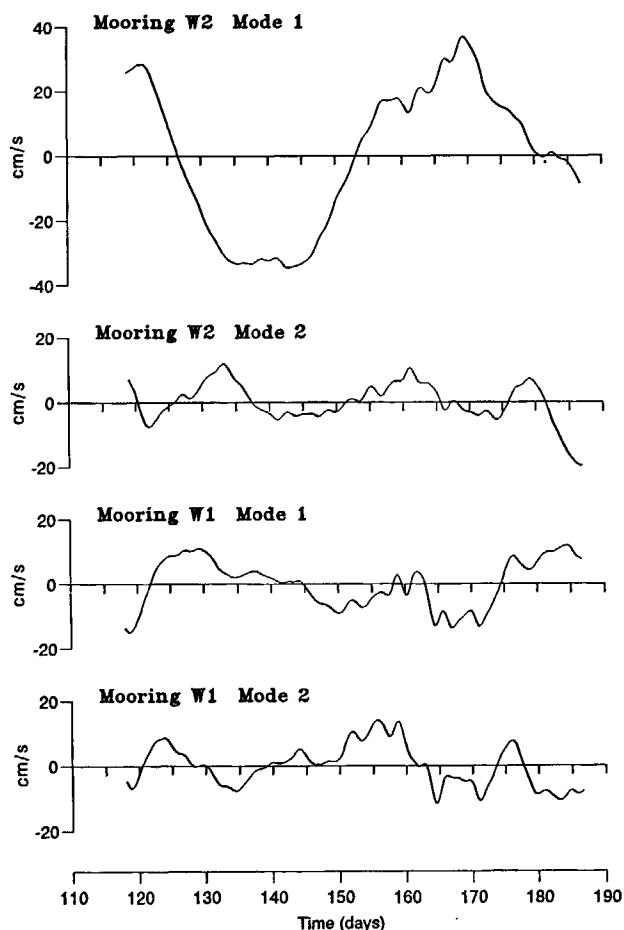


Figure 4

Expansion coefficient series of modes 1 and 2 of the EOFs for meridional current components at W1 and W2, units are arbitrary.

significant at W1 where it contributes 37 % of the variance (Tab. 2). The vertical structure (Fig. 5) of both modes is consistent with the analysis at W2. The shallowest level shows reduced amplitude because of the effect of higher frequency variability.

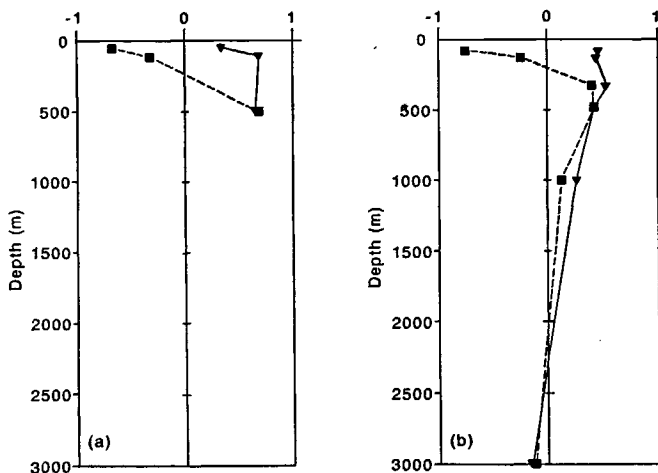


Figure 5

Eigenfunctions of the meridional components at (left) mooring W1 and (right) mooring W2. EOFs for mode 1 are represented by triangles joined by a full line and for mode 2 by squares joined by a dash line.

As the EOFs for W1 are based on only one time series from depth and two from the upper 150 m, it is not surprising that the fifty-day signal in the modal amplitudes at W1 is less apparent than at W2. The EOF results reflect the emphasis on the upper layers in the data rather than an absence of the fifty-day oscillation.

SPATIAL CURRENT MEASUREMENTS

During the two-three day passage legs to/from Aldabra (Fig. 6), continuous near-surface current measurement was undertaken using the shipboard 150 kHz ADCP. Absolute currents were calculated using satellite navigation and the ship's electromagnetic log, allowing for misalignment of the ADCP relative to the ship's heading (Pollard and Read, 1989). During the passage legs a constant speed of about 10 knots (approx. 5 m s^{-1}) was maintained and no turns were made, so gyro compass swings should be negligible. The ADCP data were despiked and interpolated to give values every 5 km, and then smoothed by applying a 21-point running mean. Currents were then depth averaged over the top 100 m to suppress small scale fluctuations and the overall mean on each leg was subtracted. Currents throughout the depth range of the ADCP (near surface to 400 m) showed similar structure.

Section A was undertaken from Mauritius to Aldabra, 13-17 April, and is about 1 000 km long. The current vectors show a wave of length between 400 and 600 km, and magnitude greater than 20 cm s^{-1} . The smaller scale variations also evident could be the signatures of mesoscale eddies (Rossby radius approximately 70 km). Section B, along the track from Aldabra to the Amirante Trench between 3-6 May, shows a distinct oscillation in the currents of amplitude 15 cm s^{-1} and apparent wavelength about 400 km. These wave amplitudes seen on sections A and B are in agreement with the magnitude of

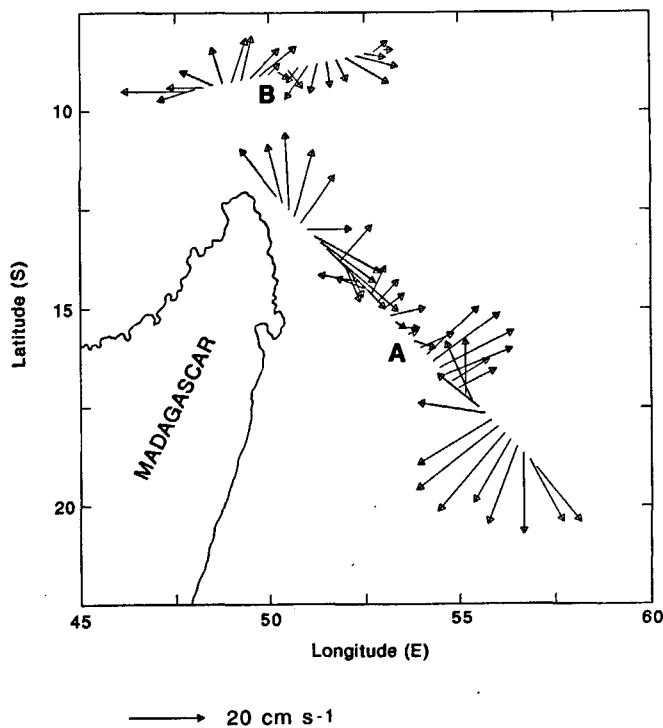


Figure 6

Passage legs A and B during which acoustic Doppler current profiler estimates of near-surface currents were obtained. Section A- Mauritius to Aldabra, 13-17 April, 1 000 km long. Section B: Aldabra to Amirante Trench, 3-6 May, 600 km long. Depth averaged ADCP currents in the upper 100 m. The mean currents for each leg have been subtracted.

the fifty-day oscillations of about 20 cm s^{-1} observed at moorings W1 and W2 in the upper few hundred metres.

SATELLITE IMAGERY

Although during the period of the experiment, no clear satellite imagery was available, a number of CZCS images in other years has been obtained. Some of these, all from the second quarter of the year, show oscillations in the South Equatorial Current. A scene from 5 May 1986 (Fig. 7 a) reveals a wave like structure in surface pigment extending northwestwards from the northern tip of Madagascar and passing close to Aldabra. The higher chlorophyll content waters seem to be associated with the current passing close to Madagascar, and are then carried downstream beside more oligotrophic waters to the north, allowing the wave to be seen on the front between the two. A similar structure is seen in the corresponding image for 30 March 1979 (Fig. 7 b). The wavelength appears to be about 250 km, somewhat shorter than indicated by the other observations. The reason for this is not clear, and there are no image sequences to allow investigation of propagation or development of the feature. The final image shown [26 April 1979 (Fig. 7 c)] shows a more cusp-like feature whose wavelength is larger, about 400 km. In all three images the wave extends in the mean direction of the South Equatorial Current at this time of year. These images provide strong evidence for the existence of wave like perturbations near Aldabra.

DISCUSSION

By correlating the meridional current components at W1 500 m and W2 480 m, where the fifty-day oscillation is clear at both sites, an estimate of its speed of propagation may be made. The correlation coefficient is 0.8 (significant at 95 % confidence level) with a lag of 150 hours; W1 leads W2, *i. e.* westward propagation. Taking the distance over which the disturbance travels in this time to be 53 km (the zonal separation between W1 and W2) yields a propagation speed of 0.1 m s^{-1} westwards. We believe this to be the first direct measurement of the propagation speed of the fifty-day oscillation.

The characteristics of the oscillation identified in the current time series are consistent with the presence of a zonally-propagating Rossby wave. For such a wave, the zonal wave number, K , is related to the frequency, w , by the dispersion equation:

$$w = \frac{-\beta K}{K^2 + \left(\frac{f^2}{gh_n}\right)}$$

where β is the latitudinal gradient of the Coriolis parameter, f , and g is gravitational acceleration. The barotropic (depth independent) mode is that with $n = 0$ and h_0 is then the water depth. The equivalent water depth is given by $h_n = \Delta\rho H/\rho$ for baroclinic (internal) modes $n = 1, 2, \text{ etc.}$ and layer depth H . We note that the phase speed is given by $c = w/K$.

If we take the first baroclinic mode, *i. e.* $n = 1$ and assume one layer 500 m thick with density difference 6 kg m^{-3} , and the phase speed of the wave, $c = 0.1 \text{ m s}^{-1}$ as calculated above, then the wavelength ($2\pi/K$) for a zonally-propagating Rossby wave at 9°S would be 425 km, and the associated period 49 days. If the wave were barotropic, taking $h_0 = 4000 \text{ m}$, then the resulting wavelength and period are not significantly different from the first mode baroclinic case. The fact that the meters at 3000 m are 180° out of phase with the near surface oscillation is evidence of the baroclinic nature of these oscillations. The waves might be generated by barotropic instability of currents trapped close to the surface, but become baroclinic on propagating away from the area of generation.

Price and Rossby (1982) discuss observations of such planetary waves in SOFAR float data at 1300 m in the western North Atlantic. Wavelength (340 km) and period (61 days) are consistent with a barotropic wave, but they include the effect of changes in topography. They note however that the gravest baroclinic mode has similar characteristics; they conclude that stratification does not strongly influence the wave. They suggest that these waves are caused by baroclinic eddies in the Gulf Stream evolving towards barotropy.

Kindle and Thompson (1989) calculate baroclinic Rossby waves in the southwest Indian Ocean to have wavelength 800 km and period 52 days (they assume a different stratification to our results). They suggest that the 400 km

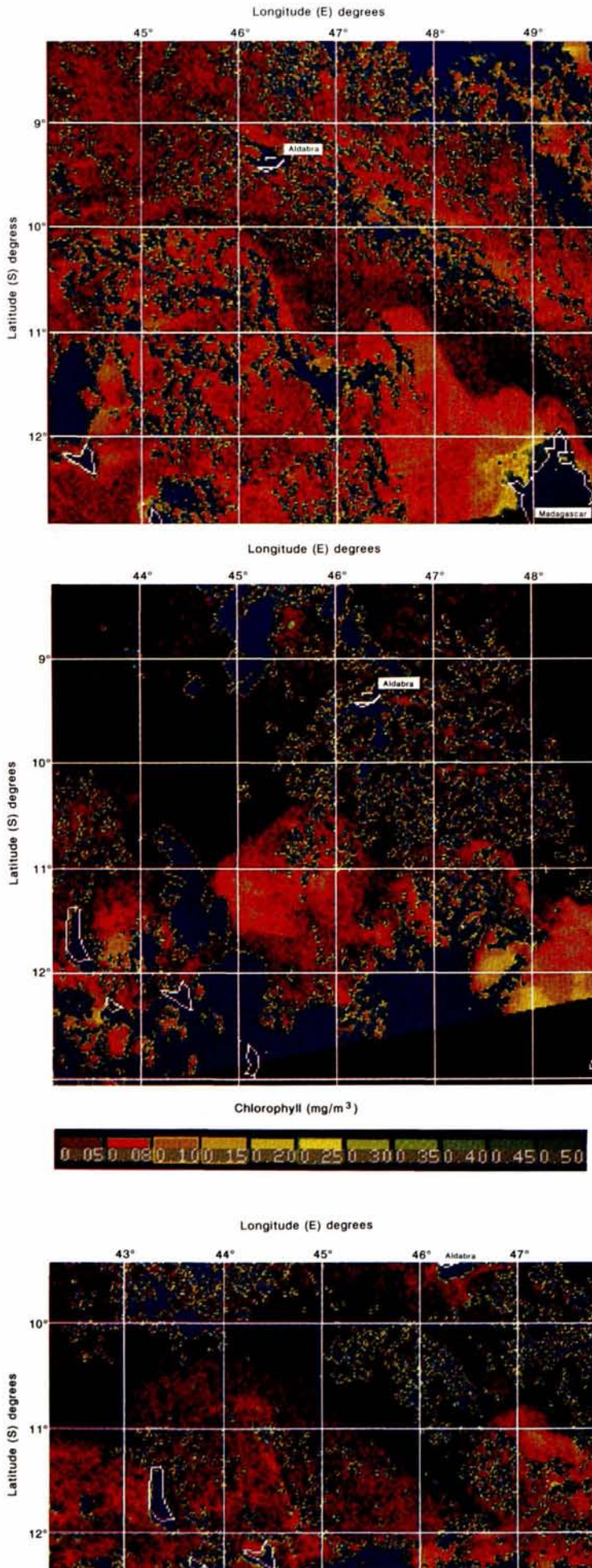


Figure 7

Coastal Zone Color Scanner images showing chlorophyll content of the surface waters. The dark blue signifies cloud or land; black denotes the lowest phytoplankton concentration. a) 5 May 1986; b) 30 March 1979; c) 26 April 1979. The colour scale is given with (c).

waves observed in the surface currents by Quadfasel and Swallow (1986) are not associated with the barotropic instability causing the fifty-day oscillation in their current meter data (and in Kindle and Thompson's one layer model), but are a manifestation of a baroclinic instability possible in westward flow away from the equator ($> 10^\circ$). Although our observations of surface current oscillations are consistent with those of Quadfasel and Swallow (1986) and are closer to the equator, it is impossible to know definitively the generation mechanism from this data set and further modelling and observations are warranted.

The estimate of the wavelength derived from the ADCP sections is unaffected by the ship's speed, 5 m s^{-1} , which is an order of magnitude greater than the phase speed of the wave, 0.1 m s^{-1} . The ADCP sampling of the wave may therefore be considered synoptic, *i.e.* any change in the apparent wavelength due to the Doppler effect is small compared to the true wavelength. If the meridional oscillations are assumed to be Rossby waves, one would expect them to be propagating westwards. During ADCP section A, the ship's heading was approximately 315° , so the apparent 600 km along-track wavelength could be corrected to a zonal wavelength of 400 km. Section B lies east-west so no correction would be necessary to the observed wavelength of 400 km.

Although there have been earlier reports of similar low frequency current oscillations in the Indian Ocean, their origin is not fully understood. Production of these forty- to sixty-day current oscillations was originally attributed to the Madden and Julian oscillation (Madden and Julian, 1972), a forty- to sixty-day oscillation in the tropical wind field (Mysak and Mertz, 1984). However, modelling results (Woodberry *et al.*, 1989; Kindle and Thompson, 1989) indicate that direct wind forcing may not be the driving mechanism. In the numerical models the area to the west of 50°E and between the Equator and 10°S is identified as one of intense eddy generation. Instabilities in the horizontal shear give rise to forty to sixty day fluctuations in the currents. The model described by Schott *et al.* (1988) shows such instabilities occurring just to the north and northwest of Madagascar. Several times each year this extended out to 55°E and to 11°S . Our observations are further north and further west.

It appears that there are preferential times of year when these waves are generated. The reduced gravity model of Kindle and Thompson (1989) showed that Rossby waves were generated by a barotropic instability associated with the east African Coastal Current, beginning around April each year (since this is a one layer model, baroclinic instabilities are not possible). The model of Schott *et al.* (1988) also showed the waves to be sporadic. Our observations happen to fall in the austral autumn and winter periods when waves are generated. Although we do not have current meter measurements from other times of year, we do have CZCS images from other seasons of the year; the images showing waves are from March, April and May. Large meanders have been seen in drifting buoy trajectories in this area (Molinari *et al.*, 1990) but there are too few to show the organised oscillation we have discussed here or to indicate any seasonal dependence.

Earlier observations of the fifty-day oscillation have been confined to single sites in coastal regions and to the upper layers. Our observations show that it also occurs away from the ocean boundaries and at depths as great as

3 000 m, and have enabled us to measure the westward propagation speed for the first time. The characteristics of the oscillation as seen in the current meter records and shipboard ADCP may be explained by a zonally propagating Rossby wave.

As was seen in the CZCS images, these waves can have important ramifications for the phytoplankton distributions in the region. Ocean colour imagery is more useful than AVHRR or ATSR imagery in observing the wave because of the uniform sea surface temperatures in the region. The future availability of improved ocean colour observations from the SeaWiFS satellite will allow further study.

Acknowledgements

This work was supported by UK Natural Environment Research Council grants GR3/5549 and GR3/7368. We are grateful to Jeff Whiting of the NASA Goddard Space Flight Center for providing the CZCS images.

REFERENCES

- Cutler A.N. and J.C. Swallow (1984) Surface currents of the Indian Ocean. Institute of Oceanographic Sciences Report No. 187, 8 pp.
- Heywood K.J., E.D. Barton and J.H. Simpson (1990) The effects of flow disturbance by an oceanic island. *J. mar. Res.*, **48**, 55-73.
- Kindle J.C. and J.D. Thompson (1989) The 26- and 50-day oscillations in the Western Indian Ocean: model results. *J. geophys. Res.*, **94**, 4721-4736.
- Kundu P., J.S. Allen and R.L. Smith (1975) Modal decomposition of the velocity field near the Oregon coast. *J. geophys. Res.*, **5**, 683-704.
- Luther M.E. and J.J. O'Brien (1985) Modelling the variability in the Somali Current, in: *Mesoscale/Synoptic Coherent Structures in Geophysical Turbulence*, J.C.J. Nihoul and B.M. Jamart, editors. Elsevier Science Publications, Amsterdam, The Netherlands.
- Luyten J.R. and D.H. Roemmich (1982) Equatorial currents at the semi-annual period in the Indian Ocean. *J. phys. Oceanogr.*, **12**, 406-413.
- Madden R.A. and P.R. Julian (1972) Description of global-scale circulation cells in the tropics with a 40-50 day period. *J. atmos. Sci.*, **29**, 1109-1123.
- Molinari R.D., D. Olson and G. Reverdin (1990) Surface current distributions in the tropical Indian Ocean derived from compilations of surface buoy trajectories. *J. geophys. Res.*, **95**, 7217-7238.
- Mysak L.A. and G.J. Mertz (1984) A 40- to 60-day oscillation in the source region of the Somali current during 1976. *J. geophys. Res.*, **89**, 711-715, 1984.
- Pollard R.T. and J.F. Read (1989) A method for calibrating ship mounted acoustic Doppler current profilers, and the limitations of gyro compasses. *J. atmos. ocean. Technol.*, **6**, 865-959.
- Price J.F. and H.T. Rossby (1982) Observations of a barotropic planetary wave in the western North Atlantic. *J. mar. Res., Suppl.*, **40**, 543 - 558.
- Quadfasel D.R. and J.C. Swallow (1986) Evidence for 50-day period planetary waves in the South Equatorial Current of the Indian Ocean. *Deep-Sea Res.*, **33**, 1307-1312.
- Schott F., M. Fieux, J. Kindle, J. Swallow and R. Zantopp (1988) The boundary currents east and north of Madagascar. 2: Direct measurements and model comparisons. *J. geophys. Res.*, **93**, 4963-4974.
- Woodberry K.E., M.E. Luther and J.J. O'Brien (1989) The wind-driven seasonal circulation in the Southern Tropical Indian Ocean. *J. geophys. Res.*, **94**, 17985-18002.
- Wyrtki K. (1973) An equatorial jet in the Indian Ocean. *Science*, **181**, 262-264.